molbank

MDPI

Short Note

1,3,3,3′,3′-Pentaisopropyl-1,3,3′,6,6′,7,7′-heptahydro-1λ5-1,1′-spirobi[acenaphtho 5,6-cd][1,2,6]oxadiphosphinine]-3,3′-diium Triiodide

Daniel Picthall [1], Matthew James Ray [2], Alexandra Martha Zoya Slawin [1] and Petr Kilian [1,*]

[1] EaStChem School of Chemistry, University of St. Andrews, St. Andrews KY16 9ST, UK
[2] Arkema UK Ltd., Clifford House, York Road, Wetherby LS22 7NS, UK
* Correspondence: pk7@st-andrews.ac.uk

Abstract: Reaction of bis(*peri*-substituted) triphosphine *i*PrP(AcenapP*i*Pr$_2$)$_2$ (Acenap = acenaphthene-5,6-diyl) with iodine, followed by hydrolysis, afforded ionic species with [*i*PrP(AcenapP(O)*i*Pr$_2$)$_2$] dication, containing P-O-P-O-P motif, balanced by triiodide anions. The new species were fully characterised, including single crystal X-ray diffraction. The formation of the unusual double-bridged motif is likely a result of crowding in the peri-region.

Keywords: phosphine; halophosphonium halide; synthesis; peri-substitution

Citation: Picthall, D.; Ray, M.J.; Slawin, A.M.Z.; Kilian, P. 1,3,3,3′,3′-Pentaisopropyl-1,3,3′,6,6′,7,7′-heptahydro-1λ5-1,1′-spirobi[acenaphtho 5,6-cd][1,2,6]oxadiphosphinine]-3,3′-diium Triiodide. *Molbank* **2022**, *2022*, M1523. https://doi.org/10.3390/M1523

Academic Editor: Rodrigo Abonia

Received: 25 October 2022
Accepted: 6 December 2022
Published: 8 December 2022

1. Introduction

The addition of halogens to phosphines produces halophosphonium halides of the general formula $[R_3PX]^+ X^-$, where X can be any of the Cl, Br, or I (Equation (1)). Halophosphoniums with trihalide anions of the general formula $[R_3PX]^+[X_3]^-$ are also known (X = Br, I); these are best prepared by the reaction of the phosphine with two equivalents of dihalogen (Equation (2)) [1].

Although usually not isolated, halophosphoniums have some important synthetic uses. For example, halophosphoniums are formed as transient intermediates in the Appel reaction, which allows the transformation of alcohols to alkyl halides. The reagents include a stoichiometric amount of triphenylphosphine and carbon tetrahalides (CCl_4, CBr_4, CI_4) as the halogen source (Equation (3)) [2].

Halophosphoniums are readily hydrolysed to phosphine oxides (Equation (4)) [3]. The reverse reaction, producing halophosphonium halides from phosphine oxide, is the key step in the catalytic version of the Appel reaction. In this more sustainable adaptation, chlorination and bromination of alcohols are performed with a catalytic amount of phosphine oxide and oxalyl halides as the halogen sources (Equation (5)) [4].

$$PR_3 + X_2 \rightarrow [PR_3X]^+X^- \quad X = Cl, Br, I \tag{1}$$

$$PR_3 + 2X_2 \rightarrow [PR_3X]^+[X_3]^- \quad X = Br, I \tag{2}$$

$$ROH + PPh_3 + CX_4 \rightarrow RCl + Ph_3P=O + CHX_3 \tag{3}$$

$$[PR_3X]^+X^- + H_2O \rightarrow R_3P=O + 2HX \tag{4}$$

$$ROH + (COCl)_2 (+ Br^- \text{ source}) \xrightarrow{Ph_3P=O\ (cat.)} RX + CO + CO_2 + HX \quad X = Cl, Br \tag{5}$$

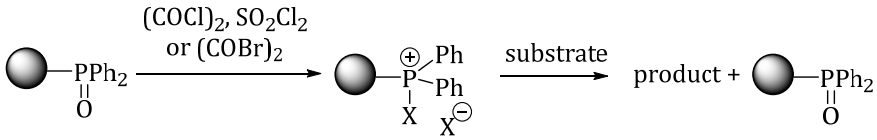

(6)

Further developments of this reactivity include using polystyrene-supported phosphine oxide, which is transformed into halophosphonium salt via reaction with oxalyl chloride or bromide. Transiently formed halophosphonium salts on polymer support are then used to effect Appel thalogenations and other dehydrative coupling reactions (Equation (6)). Using polymer-supported phosphine oxide offers major improvements in terms of purification [5,6].

In another work, P-stereogenic phosphines and their borane adducts were synthesised from phosphine oxides. This reductive pathway involves the transient formation of halophosphoniums [7]. In addition, an unusual synthetic pathway for phosphonium salts, proceeding through an electrophilic pathway, was shown to involve the transient formation of halophosphonium halides [8]. Halophosphoniums were used to study the kinetics and mechanism of nucleophilic attack on tetrahedral centres, providing proof that such attack on phosphonium centre proceeds with inversion of configuration [9,10].

In this work, we show that major steric constraints in peri-substituted phosphine led to an unusual outcome of hydrolysis of its related iodoshosphonium iodide.

2. Results and Discussion

Tridentate phosphine **1** was reacted with excess iodine in non-dried tetrahydrofuran (THF). The reaction afforded a complex mixture as confirmed by $^{31}P\{^{1}H\}$ NMR. The volatiles were removed in vacuo and replaced with acetonitrile. After cooling the acetonitrile solution, **2**$[I_3]_2$ crystallised as black rod-shaped crystals and was isolated by filtration in 31% yield. The tentative mechanism for this transformation involves the initial formation of halophosphonium species **1A**, which is hydrolysed with the residual water in the reaction solvent (THF) to afford **2**$[I_3]_2$ (Scheme 1). Carrying out the reaction in dry solvent led to a significant drop in conversion to **2**$[I]_2$, confirming that the residual water is required for the hydrolysis step.

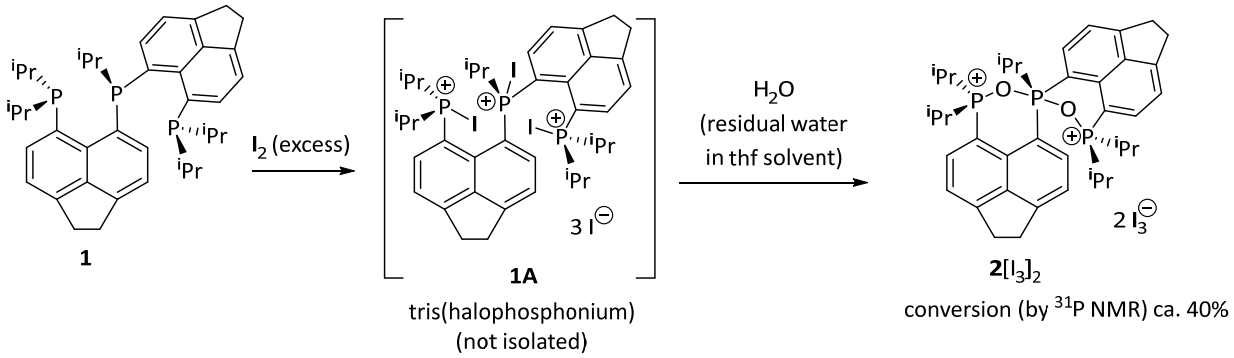

Scheme 1. Synthesis of **2**$[I_3]_2$ from tris(phosphine) **1**.

The $^{31}P\{^{1}H\}$ NMR spectrum of **2**$[I_3]_2$ consists of a triplet at δ_P −40.1 ppm corresponding to the central phosphorus atom and a doublet at δ_P 87.3 ppm corresponding to the outer phosphorus atoms, with $^{2}J_{PP}$ coupling of 33.0 Hz observed for both signals.

The crystals of **2**$[I_3]_2$ obtained from acetonitrile were subjected to single-crystal X-ray diffraction, which confirmed the connectivity, as shown in Scheme 1, as well as the presence of triiodide counterions. However, the overall quality of the **2**$[I_3]_2$ structure was rather low. Layering dark solutions of **2**$[I_3]_2$ in CH_2Cl_2 with diethyl ether yielded colourless crystals

of the diiodide salt **2**$[I]_2$, which were of better X-ray quality. For this reason, we limit the structural discussion to data obtained from **2**$[I]_2$ here.

The crystal structure of **2**$[I]_2$ (Figure 1) revealed the geometry of the two outer phosphorus atoms (P2 and P3) to be close to tetrahedral, with the bond angles around the phosphorus atoms ranging from 105.07(19) to 114.0(2)°. The central phosphorus atom is also distorted from its ideal trigonal bipyramidal geometry; the axial angle (O1-P1-O2) is 178.60(15)°, and the equatorial C-P-C angles range from 113.0(3) to 130.7(2)°.

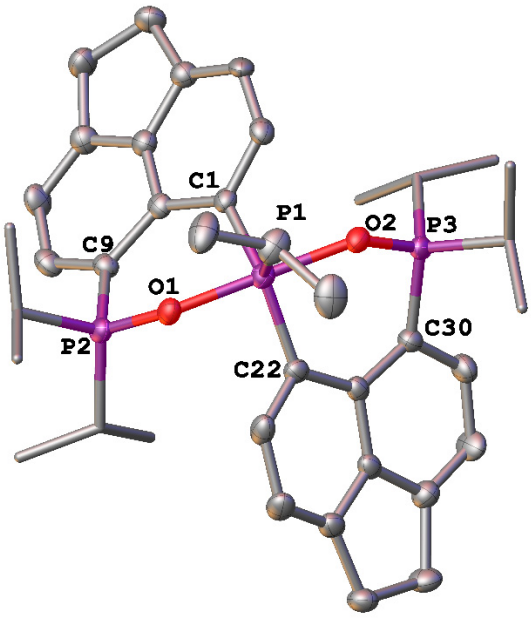

Figure 1. Molecular structure of **2**$[I]_2$ in the crystal. Anions ($2I^-$) and solvent molecules (2 CH_3CN) were omitted, and the iPr groups are shown in the wireframe for clarity. Selected bond lengths (Å), angles, and torsion angles (°): P1-O1 1.797(3), P1-O2 1.818(3), P2-O1 1.554(3), P3-O2 1.543(3), O1-P1-O2 178.60(16), C1-P1-C22 130.7(2), P1-C1···C9-P2 22.2, P1-C22···C30-P3 21.5.

It is interesting to note a large difference in the P-O bond lengths in **2**$[I]_2$. Bonds to the outer phosphorus atoms are considerably shorter (P2-O1 1.554(3) Å, P3-O2 1.543(3) Å) than those around the central phosphorus atom (P1-O1 1.797(3) Å, P1-O2 1.818(3) Å). For comparison, the P=O bond length in Ph_3PO is 1.479(2) Å [11], and axial P-O bonds in related phosphoranes range from 1.646(4) to 1.784(1) Å [12–14]. The difference in the P-O bond lengths can be interpreted as a partial double bond character of P2-O1 and P3-O2 bonds, complemented with strong dative interactions of O1 and O2 lone pairs to the central phosphorus dication ($\sigma^4P{=}O{\rightarrow}\sigma^5P^{2+}$) (structure 2′ in Figure 2). While this description appears to account for differing P-O bond lengths more readily than the all-single bonded $\sigma^4P^+{-}O{-}\sigma^5P$ phosphonium-phosphorane structure (structure 2″ in Figure 2), both of these are likely contributors to the overall bonding situation.

The structure of **2**$[I]_2$ shows the outer phosphorus atoms to be displaced much further out of the plane of their respective acenaphthene rings (P2 0.682 Å, P3 0.651 Å) than the inner phosphorus atom (0.211 Å and 0.214 Å). The angle between the two acenaphthene planes is 83°. The splay angles (+12.5(4) and +13.2(4)°) and *peri*-distances (P1···P2 3.11 Å, P1···P3 3.14 Å) are very similar for the two *peri*-regions (Note: Splay angle is a sum of the bay region angles −360°).

While thionating or selenating **1** results in a major increase in the P···P *peri*-distances [15], the formation of P-O-P bridging motifs in **2**$[I]_2$ leads to slightly reduced P···P *peri*-distances, even compared with those in the phosphine **1** (P1···P2 3.11 Å, P1···P3 3.14 Å in **2**$[I]_2$, c.f. 3.15, and 3.17 Å in **1**). At the same time, the P2···P3 distance in **2**$[I]_2$ (5.90 Å) is lengthened considerably (c.f. 4.42 Å in **1**) [15].

2$[I]_2$ was further characterised by Raman, IR, and MS (ES) spectroscopy.

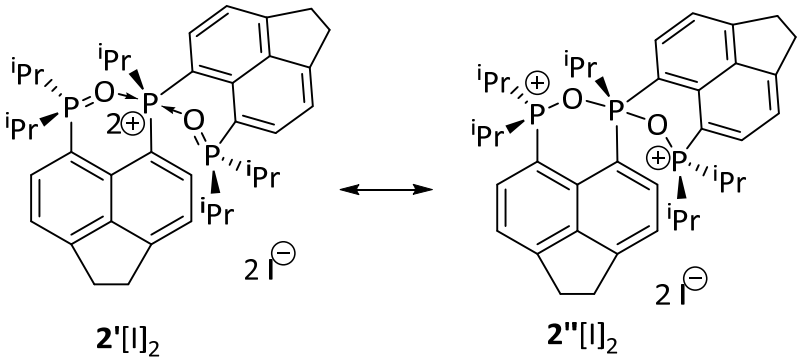

Figure 2. Bonding models for **2**$[I]_2$.

3. Conclusions

The reaction leading to the dication **2** is an interesting example of an unexpected reaction outcome due to steric crowding. While in non-crowded molecular systems, hydrolysis of halophosphoniums R_3PX^+ X^- leads invariably to phosphine oxides $R_3P{=}O$ [3], in the case of sterically crowded **1,** the middle phosphorus atom becomes oxidised; however, it does not transform to a phosphoryl group. Instead, it adopts the ionic structure shown in Figure 2, which can be interpreted either as dative interactions with the formally doubly cationic charge on the central atom **2′** or as a combination of phosphorane and double phosphonium centre **2″**. This unusual outcome is likely due to steric reasons, as the formation of the dicationic species **2** alleviates the steric pressure in the crowded peri-regions.

4. Materials and Methods

Experiments were carried out in standard Schlenk glassware under an oxygen-free nitrogen atmosphere. Tris(phoshine) **1** was synthesised using a literature procedure [15], and 85% H_3PO_4 was used as an external standard for ^{31}P NMR; ^1H NMR shifts are relative to Me_4Si, and the residual solvent peak was used for calibration ($CHCl_3$ δ_H 7.26).

I_2 (0.50 g, 0.196 mmol) was added to **1** (0.20 g, 0.326 mmol) in degassed but undried THF (10 mL) at 0 °C and allowed to warm to room temperature, leading to a dark orange suspension. The solvent was removed in vacuo to give a black oil, which was dissolved in MeCN (5 mL). **2**$[I_3]_2$ was isolated from the resulting dark orange solutions at 2 °C as large black rod-shaped crystals (0.144 g, 31.4%) (see Supplementary Materials).

E. A. (%) calculated for $C_{39}H_{51}I_6O_2P_3$: C 33.31, H 3.66; found: C 33.37, H 3.58.

^1H NMR (300.1 MHz, $CDCl_3$): δ 0.35–0.93 (br m, 15 H, *i*Pr CH_3), 1.33–1.89 (br m, 15 H, *i*Pr CH_3), 2.73–2.95 (br m, 1H, central *i*Pr CH), 3.53–3.91 (br m, 8H, CH_2 + outer *i*Pr CH), 7.65 (d, 1H, $^3J_{HH}$ = 6.8 Hz, aryl CH), 7.95 (dd, 1H, $^3J_{HP}$ = 13.4, $^3J_{HH}$ = 7.3 Hz, aryl CH), 8.35–8.44 (br m, 1H, aryl CH), 9.22 (dd, 1H, $^3J_{HP}$ = 18.7, $^3J_{HH}$ = 6.7 Hz, aryl CH).

$^{31}P\{^1H\}$ NMR (121.5 MHz, $CDCl_3$): δ −40.1 (t, inner P), 87.3 (d, outer P), $^2J_{PP}$ = 33.0 Hz.

Raman (glass capillary, cm^{-1}): 2912 (vs, υC-H), 1601 (m), 1567 (m), 1433 (s), 1319 (m), 572 (m), 176 (s).

IR (KBr disc, cm^{-1}): 2964 (m, υC-H), 1595 (s), 1453 (m), 1048 (υP-O), 855 (m), 826 (m), 630 (m), 581 (m).

MS (ES+) (*m*/*z*): 301 [Acenap(PiPr$_2$)PH], 322, 643 [Anion − H], 661 [Anion + OH], 683 [Anion + ONa].

M. p. 120–123 °C.

Supplementary Materials: The following are available online, Figure S1: ^1H and $^{31}P\{^1H\}$ NMR, IR and Raman spectra of 2$[I_3]_2$.

Author Contributions: Conceptualization, P.K. and M.J.R.; methodology, M.J.R.; crystallography, A.M.Z.S.; writing—original draft preparation, M.J.R.; writing—review and editing, P.K. and D.P.; supervision, P.K. All authors have read and agreed to the published version of the manuscript.

Funding: This research was funded by the School of Chemistry, University of St Andrews.

Data Availability Statement: The research data (NMR, IR and Raman data) supporting this publication can be accessed at https://doi.org/10.17630/90caf33b-c69c-4c71-87a0-2e1639e47247 (accessed on 24 October 2022). CCDC 2223032 contains the supplementary crystallographic data for this paper. These data can be obtained free of charge via www.ccdc.cam.ac.uk/data_request/cif, by emailing data_request@ccdc.cam.ac.uk, or by contacting The Cambridge Crystallographic Data Centre, 12 Union Road, Cambridge CB2 1EZ, UK; Fax: +44 1223 336033.

Conflicts of Interest: The authors declare no conflict of interest.

References

1. Alhanash, F.B.; Barnes, N.A.; Godfrey, S.M.; Hurst, P.A.; Hutchinson, A.; Khan, R.Z.; Pritchard, R.G. Structural isomerism in tris-tolyl halo-phosphonium and halo-arsonium tri-halides, [(CH3C6H4)3EX][X3], (E = P, As; X = Br, I). *Dalton Trans.* **2012**, *41*, 7708–7728. [CrossRef] [PubMed]
2. Appel, R. Tertiary Phosphane/Tetrachloromethane, a Versatile Reagent for Chlorination, Dehydration, and P—N Linkage. *Angew. Chem. Int. Ed. Engl.* **1975**, *14*, 801–811. [CrossRef]
3. Quin, L.D. *A Guide to Organophosphorus Chemistry*; Wiley Interscience: New York, NY, USA, 2000.
4. Denton, R.M.; An, J.; Adeniran, B.; Blake, A.J.; Lewis, W.; Poulton, A.M. Catalytic Phosphorus(V)-Mediated Nucleophilic Substitution Reactions: Development of a Catalytic Appel Reaction. *J. Org. Chem.* **2011**, *76*, 6749–6767. [CrossRef] [PubMed]
5. Tang, X.; An, J.; Denton, R.M. A procedure for Appel halogenations and dehydrations using a polystyrene supported phosphine oxide. *Tetrahedron Lett.* **2014**, *55*, 799–802. [CrossRef]
6. Xia, X.; Toy, P.H. Rasta resin–triphenylphosphine oxides and their use as recyclable heterogeneous reagent precursors in halogenation reactions. *Beilstein J. Org. Chem.* **2014**, *10*, 1397–1405. [CrossRef] [PubMed]
7. Rajendran, K.V.; Gilheany, D.G. Identification of a key intermediate in the asymmetric Appel process: One pot stereoselective synthesis of P-stereogenic phosphines and phosphine boranes from racemic phosphine oxides. *Chem. Commun.* **2012**, *48*, 10040–10042. [CrossRef] [PubMed]
8. Vetter, A.C.; Nikitin, K.; Gilheany, D.G. Long sought synthesis of quaternary phosphonium salts from phosphine oxides: Inverse reactivity approach. *Chem. Commun.* **2018**, *54*, 5843–5846. [CrossRef] [PubMed]
9. Nikitin, K.; Jennings, E.V.; Al Sulaimi, S.; Ortin, Y.; Gilheany, D.G. Dynamic Cross-Exchange in Halophosphonium Species: Direct Observation of Stereochemical Inversion in the Course of an SN2 Process. *Angew. Chem. Int. Ed.* **2018**, *57*, 1480–1484. [CrossRef] [PubMed]
10. Jennings, E.V.; Nikitin, K.; Ortin, Y.; Gilheany, D.G. Degenerate Nucleophilic Substitution in Phosphonium Salts. *J. Am. Chem. Soc.* **2014**, *136*, 16217–16226. [CrossRef] [PubMed]
11. Al-Farhan, K.A. Crystal structure of triphenylphosphine oxide. *J. Crystallogr. Spectrosc. Res.* **1992**, *22*, 687–689. [CrossRef]
12. Chandrasekaran, A.; Day, R.O.; Holmes, R.R. Isomeric Intraconversion among Penta- and Hexacoordinate Cyclic Oxyphosphoranes via Oxygen Atom Coordination 1,2. *J. Am. Chem. Soc.* **1997**, *119*, 11434–11441. [CrossRef]
13. Jiang, X.-D.; Matsukawa, S.; Yamamichi, H.; Kakuda, K.-i.; Kojima, S.; Yamamoto, Y. Stereomutation and Experimental Determination of the Relative Stability of Diastereomeric O-Equatorial Anti-Apicophilic Spirophosphoranes. *Eur. J. Org. Chem.* **2008**, *2008*, 1392–1405. [CrossRef]
14. Chandrasekaran, A.; Day, R.O.; Holmes, R.R. Coordination of Carbonyl and Carboxyl Oxygen Atoms with Phosphorus in the Presence of Hydrogen Bonding. P−O Donor Action. *Inorg. Chem.* **2001**, *40*, 6229–6238. [CrossRef]
15. Ray, M.J.; Randall, R.A.M.; Arachchige, K.S.A.; Slawin, A.M.Z.; Buehl, M.; Lebl, T.; Kilian, P. Synthetic, Structural, NMR, and Computational Study of a Geminally Bis(peri-substituted) Tridentate Phosphine and Its Chalcogenides and Transition-Metal Complexes. *Inorg. Chem.* **2013**, *52*, 4346–4359. [CrossRef] [PubMed]